Zagazig University Medical Journal
www.zumj.journals.ekb.eg

https://doi.org/10.21608/zumj.2023.209146.2796 Volume 29, Issue 4, Jully 2023

Manuscript ID ZUMJ-2305-2796 (R1)
DOI 10.21608/zumj.2023.209146.2796

ORIGINAL ARTICLE

Asprosin, a Prospective Biomarker for Rhabdomyolysis-Induced Acute Kidney Damage in Rats: Involvement of PKA/TGF-β1/SMAD-3 Signaling Pathway

Sama S. Khalil[1*], Samaa Salah Abd El-Fatah[2], Maha Abdelhamid Fathy[1], Nisreen E. Elwany[3], Enssaf Ahmad Ahmad[2], Noura Mostafa Mohamed[4], Marwa A. Habib[1]

[1]Medical Physiology Department, Faculty of Medicine, Zagazig University, Egypt
[2]Human Anatomy and Embryology Department, Faculty of Medicine, Zagazig University, Egypt
[3]Clinical Pharmacology Department, Faculty of Medicine, Zagazig University, Egypt
[4]Medical Biochemistry Department, Faculty of Medicine, Zagazig University, Egypt

***Corresponding author:**
Sama S. Khalil
sskhaleel@medicine.zu.edu.eg,
Dr.samakhalil@gmail.com

Submit Date	2023-05-05 18:44:53
Revise Date	2023-05-25 14:43:51
Accept Date	2023-05-26

ABSTRACT

Background: Rhabdomyolysis is a primary skeletal muscle disruption syndrome with circulatory leakage of its intracellular contents and is seriously complicated by acute kidney injury (AKI). Asprosin is a novel glucogenic adipokine expressed in several tissues, including the kidneys, and has been implicated in some renal disorders via many pathogenic mechanisms. ***Methods:*** 32 rats were divided equally into the control group, the calcitriol-treated group, the glycerol-treated group, and the glycerol+calcitriol-treated group. Blood, urine, and renal tissue samples were collected for biochemical, histological, immunohistochemical, and gene investigations. ***Results:*** Rats given glycerol had elevated levels of asprosin, creatine kinase, creatinine, BUN, renal MDA, IL-6, caspase-3, and caspase-9, as well as PKA mRNA, TGF-β1, and SMAD-3. While creatinine clearance, renal SOD, and catalase were decreased. Marked histopathological changes imply sever renal injury, faint PAS-positive reaction, strong positive immunoreaction for iNOS and TGF-β were found. These changes were reversed in glycerol+calcitriol-treated rats. Asprosin positively correlated with MDA, IL-6, caspase-3, caspase-9, mRNA levels of PKA, TGF-β1and SMAD-3, while it negatively correlated with SOD, and catalase. ***Conclusion:*** Serum asprosin levels are increased in rhabdomyolysis-induced AKI and calcitriol protect against AKI via suppressing asprosin and its dependent PKA-TGF-β1-SMAD-3 signaling pathway.

Keywords: Rhabdomyolysis; asprosin; acute kidney injury; TGF-β1

INTRODUCTION

Rhabdomyolysis is a clinical condition characterized by primary muscular damage and leakage of intracellular muscle contents into the circulation. It is usually caused by muscular trauma, as in road traffic accidents, although it can also happen under non-traumatic circumstances such as those brought on by strenuous exercise, infections, continuous muscular compression, and toxicity exposure [1]. Acute kidney injury (AKI) is the most serious and common complication, with a high mortality rate [2]. The pathogenesis of AKI by rhabdomyolysis involves the precipitation of leaked myoglobin in renal tubules, inducing tubular necrosis, and the resultant cell debris occludes renal tubular fluid flow with enhancement of oxidative stress and renal vasoconstriction [3].

Rhabdomyolysis-associated AKI is easily induced experimentally in rats by intramuscular injection of glycerol since they exhibit stable functional and morphological renal abnormalities [4]. A complex pathogenesis was reported by several studies for glycerol-induced AKI and involved the toxicity of myoglobin released from damaged muscles, inflammation, oxidative stress, and apoptosis [5].

Asprosin, a small 30 kDa protein with 140 amino acids, was recently identified as a glucogenic adipokine that regulates carbohydrate and lipid metabolism [6]. Asprosin is encoded by two exons of the FBN1 gene and is formed by cleavage of the C-terminus of the fibrillin-1 protein [7].

A recent study detected the presence of asprosin in other tissues such as the kidneys, liver, heart, brain, testicles, and stomach [8]. Asprosin has been shown to have an inflammatory effect as it correlated positively with inflammatory cytokines and upregulated the inflammatory JNK phosphorylation TLR4-dependent pathway [9]. Also, it was found that increased levels of circulating asprosin were associated with diabetic nephropathy and that asprosin may affect renal homeostasis via several pathogenic mechanisms

such as inflammation, insulin resistance, and endothelial dysfunction [9-11].

The cytokine transforming growth factor-beta (TGF-β) has been demonstrated to regulate several cellular processes, including apoptosis, and the pathogenesis of fibrosis [12]. TGF-β1 was found to be increased in renal injury induced in glycerol-treated rats [13]. Also, it was reported to participate in renal interstitial fibrosis by inducing tubular epithelial-to-mesenchymal transition [14].

A recent study revealed that asprosin directly induces endothelial-to-mesenchymal transition (EndoMT) in diabetic lower extremity peripheral artery disease via activation of the TGF-β signaling pathway [15]. Also, it was reported that aerobic exercise training decreased asprosin-dependent protein kinase A (PKA)/TGF-β levels in the liver of streptozotocin-induced diabetic rats [16].

1,25-dihydroxyvitamin D3 (calcitriol) has been shown to protect the kidney by suppressing pro-inflammatory and pro-fibrotic factors and oxidative stress pathways [17]. Additionally, calcitriol was reported to ameliorate renal structural and functional changes induced by glycerol via attenuating inflammatory processes and oxidative damage [18]. Moreover, the protective effect of calcitriol against fibrosis in diabetic nephropathy was found to be mediated via inhibition of TGF-β1 [19].

However, to our knowledge, there are no reports showing changes in asprosin levels in rhabdomyolysis-associated AKI. Therefore, the present study was conducted to assess serum asprosin levels in glycerol-treated rats and their relationship with changes in renal functional, oxidative, apoptotic, and inflammatory parameters. Secondly, to investigate the role of the PKA-TGF-β1-SMAD-3 signaling pathway, and its relation to asprosin. Lastly, to explore whether pretreatment with calcitriol could protect against acute kidney injury via suppressing asprosin and its downstream dependent mechanisms.

METHODS

Ethical statement

The experimental procedures were conformed to the National Institutes of Health guide for care and use of experimental animals and were approved by Zagazig University committee for animal care and use (ZU-IACUC/3/F/328/2022).

Animals and experimental design

Thirty-two male albino rats, weighing 170-190 g were purchased from the Faculty of Veterinary Medicine, Zagazig University, then housed 4 animals/cage in steel wire cages (50 cm x 30 cm x 20 cm) under hygienic conditions at room temperature in Physiology Department Animal House, Faculty of Medicine, Zagazig University and maintained on a 12-hour dark/light cycle. Before the start of experiments, rats were kept for 2 weeks to accommodate animal house conditions and were allowed free access to food, but were deprived of drinking water for 24 hours before glycerol injection and 1 hour after injection.

The animals were divided randomly into four equal groups of eight rats each, as follows: Control group; in which rats were injected intraperitoneally (i.p.) with 0.1 ml castor oil once daily for seven days, then injected intramuscularly (i.m.) with saline (10 mL/kg) on the seventh day, and half the dose was administered to each hind limb muscle, Calcitriol (Calc)-treated group, in which rats were injected i.p. with calcitriol (0.5 µg/kg), diluted in castor oil once daily for seven days [20], then injected i.m. with saline (10 mL/kg) on the seventh day, and half the dose was administered to each hind limb muscle, Glycerol (Glyc)-treated group; in which rats were injected i.p. with 0.1 ml castor oil once daily for seven days, then injected i.m. with 50% glycerol (10mL/kg) diluted in saline on the seventh day [21], half the dose was administered to each hind limb muscle, Glycerol+Calcitriol (Glyc+Calc)-treated group; in which rats were injected i.p. with calcitriol (0.5 µg/kg), diluted in castor oil once daily for seven days, then were injected i.m. with 50% glycerol (10 mL/kg) diluted in saline on the seventh day, half the dose was administered to each hind limb muscle and the last dose of calcitriol was given one hour before glycerol injection. Calcitriol was bought in the form of Devarol-S (200000 IU;5000 µg/2ml ampoule) from Memphis Pharmaceuticals & Chemical Industries Co., Egypt; while glycerol was bought from El-Gomhuria Co. Cairo, Egypt.

After glycerol injection, rats were kept for 48 hours with free access to water, and diet. On the ninth day, rats were transferred to metabolic cages, and 24- hour urine was collected. On the tenth day, all rats were anesthetized with thiopental sodium (60 mg/kg, i.p). After anesthesia, blood was collected via retro-orbital puncture, then a midline abdominal incision was performed in all animal groups and their kidneys were harvested for biochemical, gene expression, histological, and immunohistochemical analysis.

Blood sampling: The collected blood was left for 30 minutes at room temperature to allow clotting. Serum was separated by centrifugation of the supernatant of clotted blood samples for 15 minutes at 3000 rpm then stored at -20°C until use for estimation of biochemical parameters.

Urine sampling: On the ninth day, rats were individually housed in metabolic cages in which suitable-sized funnels with perforated plastic discs were settled at their bottoms to allow urine

collection while retaining the feces. The 24-hour urine for each animal was collected in a beaker, the volume was measured, and then insoluble materials were removed by centrifugation for 10 minutes at 3000 rpm. The supernatant was stored at -20ºC until biochemical analysis.

Renal tissue preparation for biochemical analysis: the right kidney from each animal was harvested, rinsed with ice-cold saline, and then gently homogenized with homogenization buffer (10 mM Tris-HCl, 1 mM EDTA, pH 7.4). The resulting homogenates (10% w/v) were then centrifuged at 5000 rpm for 10 min at 4 °C. The supernatant was then used for analysis of renal oxidative, inflammatory, and apoptotic parameters.

Biochemical analysis:

1. Assessment of kidney function: Serum samples were examined for creatinine and blood urea nitrogen, (BUN) and urine samples were examined for urine creatinine spectrophotometrically using colorimetric commercial kits (Biomerieux, Marcy l'Etoile, France) following the manufacturer's instructions. The calculation of urine flow in ml/min was attained by dividing the volume of 24-hour urine by 1440. Then, creatinine clearance in ml/min was calculated using the formula "Creatinine clearance = [urine creatinine (mg/dl) × urine flow (ml/min)] / serum creatinine (mg/dl)" [22].
2. Assessment of serum asprosin and creatine kinase (CK)**:** Serum asprosin levels were measured using enzyme-linked immunosorbent assay (ELISA) kits (Catalog No. ER1944) based on the manufacturer's protocol. CK was analyzed using commercial kits that were purchased from Biodiagnostic-Egypt (Catalog No. MBS2515061) following the manufacturer's protocol.
3. Assessment of renal lipid peroxidation and antioxidant enzymes: According to the supplier's instructions, the corresponding kits (Jiancheng, Nanjing, China) were used to quantify the levels of the lipid peroxidation marker malondialdehyde (MDA)(A003) and the levels of the antioxidant enzymes superoxide dismutase (SOD) (A001-2-2) and catalase (A007-1-1) in renal tissue with the help of UV-Visible spectrophotomer (ELICO Limited).
4. Assessment of renal inflammation and apoptosis index: Kidney tissue inflammatory marker Interleukin-6 (IL-6) was measured using the RayBio Rat IL-6 ELISA Kit (RayBiotech, Inc. Norcross, GA). Renal concentrations of apoptotic markers; caspase-3 and caspase-9, were measured using Rat Caspase-3 and Caspase-9 ELISA Kits (Cusabio Biotech, Hubei, China) respectively, following the instructions from the manufacturer. The end reactions for caspase-3 and caspase-9 were quantified by PNA light emission as measured at 405 nm using an ELISA reader (ELx 800TM BioTek, USA).

Quantitative real-time PCR of PKA, TGF-β1 and SMAD-3:

Total RNA from renal tissue was extracted by Trizol reagent, and the integrity of the RNA was tested on 2% agarose gels. Further, the concentration of total RNA was measured by a spectrophotometer (Thermo, Waltham, MA, USA). The RNA (2 µg / sample) was reverse transcribed into cDNA by a quantitative real-time PCR machine (ABI-7300, USA) using SYBR Green reagents (Thermo, USA). All primers (Table 1) for the real-time PCR were designed by Primer 5.0 and synthesized by JRDun Biotech (Shanghai, China). Relative mRNA expression was evaluated by $2^{-\Delta\Delta CT}$ relative quantitative analysis in each sample against GAPDH gene expression.

Histological assessment by light microscope:

Left kidney samples were embedded in paraffin after being fixed in 10% buffered formalin. Hematoxylin and eosin (H&E) staining and the periodic acid Schiff reaction (PAS) were applied to serial slices that ranged in thickness from 5-7 µm [23]. For immuno-histochemical labeling, a rabbit monoclonal antibody of the IgG subclass was used to specifically localize the oxidative stress marker, inducible nitric oxide synthase (iNOS) and identify transforming growth factor (TGF-β1) in paraffin sections. The kits came from ABclonal Biotechnology and have catalog numbers A14031 for iNOS and A16640 for TGF-β1. Following the manufacturer's recommendations, the technique protocol was standardized, as previously described [24]. At Zagazig University's Faculty of Medicine's Human Anatomy and Embryology Department, a light microscopic examination was conducted using an LEICA DM500. The Endothelial, Glomerular, Tubular, and Interstitial (EGTI) scoring system was used to assess the histopathological alterations in renal tissue (Table 2) [25].

STATISTICAL ANALYSIS

If the data were normally distributed, continuous variables were given as the mean standard error (SEM). The Kolmogorov-Smirnov test served as a model for normality. The one-way ANOVA was used to identify significant group differences. Tukey's post hoc test was used to compare groups. The median and interquartile range was used to describe continuously skewed data (IQR). Where equal variances weren't present, the Kruskal-Wallis test and Dunn's multiple comparison tests were applied. $P<0.05$ was settled for significance of all statistical tests. The Graph Pad Prism software, version 5.0, was used to

identify statistical group differences (Graph Pad Software, San Diego, CA, USA). Pearson's correlation coefficient analysis was done by SPSS software program, version 19 to determine possible relationship between serum asprosin levels and the other measured parameters **(**SPSS Inc. Chicago, IL, USA).

RESULTS

Serum levels of asprosin:

As represented in Fig. 1A, glycerol injection significantly increased serum asprosin levels in comparison to control and Calc-treated groups, while pretreatment with calcitriol in the Glyc+Calc group induced a significant reduction in serum asprosin levels compared to Glyc-treated rats. However, no significant difference in asprosin levels was detected between control and Calc-treated rats.

Serum levels of creatine kinase:

The data in Fig. 1B showed that injection of glycerol in the Glyc-treated group significantly increased serum creatine kinase levels compared with the control and Calc-treated groups. Pretreatment with calcitriol in Glyc+Calc group had no significant effect on serum creatine kinase levels compared with the Glyc-treated group, but they still significantly increased compared with the control and Calc-treated groups.

Modification of renal functioning characteristics:

As presented in Figs. 1C, D, and E, injection of glycerol induced a statistically significant increase in serum creatinine and serum BUN but a significant decrease in creatinine clearance in comparison to the control and Calc-treated groups. While, pretreatment with calcitriol in the Glyc+Calc group induced a significant decrease in serum creatinine and BUN but a significant rise in creatinine clearance when compared with Glyc-treated rats. Conversely, there was a statistically insignificant difference in levels of the previous parameters between control and Calc-treated rats.

Modifications in the renal oxidative parameters:

As shown in Figs. 2A, B, and C, glycerol injection significantly increased renal tissue concentrations of MDA, but significantly decreased concentrations of SOD and catalase in comparison to control and Calc-treated groups. Meanwhile, pretreatment with calcitriol in the Glyc+Calc group induced a statistically significant decrease in MDA concentration, but a significant rise in SOD and catalase as compared with Glyc-treated rats. On the other hand, no statistically significant difference in levels of the previous parameters was detected between control and Calc-treated rats.

Modifications of apoptotic and inflammatory markers in the kidneys:

As expressed in Figs. 2D, E, and F, glycerol injection significantly increased renal tissue concentrations of the apoptotic markers caspase-3&caspase-9 and the inflammatory marker IL-6 in comparison to the control and Calc-treated groups. While pretreatment with calcitriol in Glyc+Calc group induced a statistically significant decrease in the concentration of the previous parameters as compared with the Glyc-treated group. Conversely, no statistically significant difference in levels of the previous parameters was detected between control and Calc-treated rats.

Changes in the levels of PKA, TGF-β, and SMAD-3 mRNA expression in the kidneys:

As noticed in Fig. 3, mRNA expression levels of PKA, TGF-β1, and SMAD-3 were significantly up-regulated in rats treated with glycerol compared with control and Calc-treated groups. While the mRNA expression levels of those parameters were significantly down-regulated by calcitriol pretreatment in the Glyc+Calc-treated group as compared to Glyc-treated rats, there was no statistically significant difference in the mRNA expression levels of the previous parameters between control and Calc-treated rats.

Correlation between asprosin serum levels and the other studied parameters:

As demonstrated in Table 3, statistically significant positive correlations were found between serum levels of asprosin and renal tissue levels of MDA, caspase-3, caspase-9, IL-6, mRNA of PKA, TGF-β1, and SMAD-3, while they were negatively correlated with SOD and catalase in both Glyc and Glyc+Calc-treated groups. On the other hand, no significant correlation was detected between asprosin and any of the previous parameters in either the control or Calc-treated groups.

Renal histopathogical findings

H&E- stained sections of the renal cortex of control rats showed normal renal corpuscles, proximal and distal convoluted tubules (PCT and DCT, respectively) with minimal interstitium. Each renal corpuscle consisted of a glomerulus surrounded by Bowman's capsule, enclosing Bowman's space (Fig. 4A.a,e). Histological examination of the renal tissues of Calc-treated rats showed similar morphological results. So this group was considered congruent with the control group (Fig. 4A.b,f).

Glyc-treated renal cortex showed shrunken, segmented glomeruli with widened Bowman’s spaces. A dilated tubular system was obvious, and some tubules appeared distorted with the absence of their brush border. Many hyaline casts obliterated their lumina. Other ones appeared

necrotic. The interstitium revealed infiltrating inflammatory cells, areas of hemorrhage, and dark stained pyknotic nuclei. There were thickened-wall blood vessels within the interstitium (Fig. 4A.c,g).

On the other hand, in the Glyc+Calc-treated group, there was an obvious improvement in the histological structure of renal cortical tissues. The glomeruli were surrounded by normal parietal and visceral layers of Bowman's capsule, enclosing Bowman's space. PCT were lined by tubular cells with vesicular nuclei and an intact brush border, except for a few tubules that revealed casts. Some DCT were normal except for a few tubules that showed pyknotic nuclei in their lining. A nearly normal interstitium was seen except for some apoptotic nuclei and limited areas of hemorrhage (Fig. 4A.d, h).

Morphometrically, regarding the renal corpuscles in the Glyc-treated group, there was a significant decrease in the area of the glomerular capillary tuft and a significant increase in the thickness of Bowman's space when compared with the control and Calc-treated groups.

While the Glyc+Calc-treated group revealed a significant increase in the area of the glomerular capillary tuft and a significant decrease in the Bowman's space thickness when compared to the Glyc-treated rats, yet the Glyc+Calc-treated group showed a significant increase in glomerular tuft area and a decrease in Bowman's space thickness when compared to the control and Calc-treated rats (Fig. 4B, C).

Furthermore, morphometric measurements of the diameters of both PCT and DCT in the Glyc-treated group showed a significant increase when compared with the control and Calc-treated groups. On the contrary, the Glyc+Calc-treated group revealed restoration of normal tubular structure, and these results were emphasized by the morphometric measurements of both PCT and DCT, which recorded a significant decrease in their diameters as compared to the Glyc-treated group and an insignificant difference as compared to the control and Calc-treated groups (Fig. 4D,E).

The periodic acid Schiff (PAS)- stained sections of the control and Calc-treated renal cortex revealed positive reactions at the basal lamina of the glomerular capillary endothelium, basement membrane of tubules, and the brush border of PCT (Fig. 5A.a,b). A faint PAS-positive reaction was detected at the basal lamina of the glomerular capillary endothelium, tubular cells, and interrupted brush border of PCT in the Glyc-treated group (Fig. 5A.c).

PAS-stained sections of the Glyc+Calc-treated group revealed a normalized positive reaction at the basal lamina of the glomerular capillary endothelium, tubular cells, and the brush border of some PCT as compared to the control group (Fig. 5A.d).This was proved statistically by comparing the optical density of PAS among various groups.

In the Glyc-treated group, the PAS optical density revealed a significant decrease compared to the control group. The administration of calcitriol with glycerol caused a significant increase in PAS optical density compared to the Glyc-treated group. While there was no statistically significant difference between the control, Calc-treated, and Glyc+Calc-treated groups (Fig. 5B).

Renal immunohistochemistry findings

Immunohistochemical staining for iNOS immunoreaction in control and Calc-treated groups revealed a faint positive immunoreaction in the cytoplasm of renal tubular cells. While negative immunoreaction was shown in the cytoplasm of the glomerular capillary endothelium (Fig. 5A.e, f).

A strong positive immunoreaction was detected in the cytoplasm of renal tubular cells and some capillary endothelial cells in rats treated with glycerol (Fig. 5A.g). In the Glyc+Calc-treated group, weak positive immunoreactions were observed in the cytoplasm of renal tubular cells and in the cytoplasm of glomerular capillary endothelium (Fig. 5A.h).

A statistically significant increase in the mean area percentage of iNOS immunoreaction was detected in the Glyc-treated group as compared to the control and Calc-treated groups. In Glyc+Calc-treated group, there was a significant decrease in the mean area % of iNOS immunoreaction compared to Glyc-treated group, but it still revealed a significant difference as compared to the control and Calc-treated groups (Fig. 5C).

The immunohistochemical reaction for TGF-β in the control and Calc-treated groups showed a minimal positive cytoplasmic reaction in the tubular epithelial cells (Fig. 5A.i,j). The tubular cells showed a strong positive reaction in the Glyc-treated group (Fig. 5A.k). On the other hand, tubular epithelial cells of Glyc+Calc-treated group showed a mild positive cytoplasmic reaction (Fig. 5A.l). These results proved a statistical difference on comparing the mean area % of TGF-β immunoexpression among groups. Glycerol-administrated rats showed a significant increase when compared to the control group. On the contrary, administration of calcitriol with glycerol caused a significant decrease when compared to Glyc-treated group. No statistically significant difference was detected between control, Calc-treated and Glyc+Calc-treated groups (Fig. 5D).

The EGTI histopathological scoring findings

As demonstrated in Table 4, the scoring system involved the histological lesion in four individual components of the renal cortex: Tubular, Glomerular, Endothelial, and Interstitial. The evaluation of the Glyc-treated group showed varying degrees of damage to the renal cortex. It was presented by marked tissue loss with necrosis and disrupted brush border up to 60% plus cast formation (Tubular score 3). Additionally, there was widening in Bowman's space related to the retraction of the glomerular tuft (glomerular score 2). Inflammation and hemorrhage within the interstitial space, with necrosis in up to 60% of the cells (interstitial score 3), were obvious. Endothelial disturbance was recorded (endothelial score 2). All of these parameters showed significant differences as compared to the control and Calc-treated groups. Concerning the Glyc+Calc-treated group, there was an obvious improvement on the scoring system, as noted by the normalized brush border of the tubular cells in about 75% of specimens and a decrease in the areas of inflammation and hemorrhage in less than 25% of the interstitial compartment with absent necrosis. Glomeruli showed widening of bowman space (Glomerular score 1). All of these parameters showed significant differences ($p<0.001$) as compared to the Glyc-treated groups and ($p<0.05$) as compared to the control and Calc-treated groups.

Table 1: Primer sequences used for qPCR

mRNA rat Primer sequence	
PKA	5′-TAAACCGGTTCACAAGGCGTG-3′ 5′-GTTACCAACGCATCTTCCAAC-3′
TGF-β1	5′-CAATTCCTGGCGTTACCTTG 5′-AAAGCCCTGTATTCCGTCTC
SMAD-3	5′-GCCTGTGCTGGAACATCATC-3′ 5′-TTGCCCTCATGTGTGCTCTT-3′
GAPDH	5′-GGAGTCTACTGGCGTCTTCAC 5′-ATGAGCCCTTCCACGATGC

Table 2: The Endothelial, Glomerular, Tubular, and Interstitial (EGTI) scoring system

Tissue type	Damage	Score
Tubular	No damage	0
	Loss of brush border (BB) in less than 25% of tubular cells. Integrity of basal membrane	1
	Loss of BB in more than 25% of tubular cells. Thickened basal membrane	2
	(Plus) Inflammation, cast formation, Necrosis up to 60% of tubular cells	3
	(Plus) Necrosis in more than 60% of tubular cells	4
Endothelial	No damage	0
	Endothelial swelling	1
	Endothelial disruption	2
	Endothelial loss	3
Glomerular	No damage	0
	Thickened Bowman capsule	1
	Retraction of glomerular tuft	2
	Glomerular fibrosis	3
Tubulo/Interstitial	No damage	0
	Inflammation and hemorrhage less than 25%nof the tissue	1
	(Plus) necrosis in less than 25% of tissue	2
	Necrosis up to 60% of tissue	3
	Necrosis more than 60% of tissue	4

Image J analysis software (Fiji image j; 1.51 n, NIH, USA) was used to measure the thickness of Bowman's space (um), Area of capillary tuft (um^2) and diameters of proximal and distal convoluted tubules (um) in 5 different fields per section, stained with H&E at (X400). After immunostaining, analysis of optical density of PAS and mean area % of iNOS and TGF-β1 were analyzed in 5 different fields per section from each animal/group. The findings were statistically analyzed.

Table 3: Pearson's correlation coefficient between serum asprosin levels and the other parameters in all studied groups

Parameters	Correlations with asprosin			
	Control	Calc	Glyc	Glyc+Calc
Serum creatine kinase	0.560	0.636	0.694	0.116
Serum creatinine	0.367	0.350	0.641	0.192
Serum BUN	0.324	0.219	0.116	0.021
Creatinine clearance	0.656	0.403	0.614	0.658
Renal MDA	0.586	0.001	0.750*	0.844**
Renal SOD	0.468	0.470	-0.938**	-0.836**
Renal catalase	0.260	0.446	-0.916**	-0.938**
Renal caspase-3	0.682	0.296	0.877**	0.814*
Renal caspase-9	0.152	0.427	0.896**	0.936**
Renal IL-6	0.496	0.599	0.939**	0.842**
Renal mRNA of PKA	0.657	0.659	0.893**	0.921**
Renal mRNA of TGF-β1	0.514	0.644	0.821*	0.914**
Renal mRNA of SMAD-3	0.653	0.457	0.833*	0.943***

BUN; blood urea nitrogen, MDA; malondialdehyde, SOD; superoxide dismutase, IL-6; interleukin-6, PKA; protein kinase A, TGF-β1; transforming growth factor-beta 1, Calc; calcitriol-treated, Glyc; glycerol-treated, Glyc+Calc; glycrol+calcitriol-treated. *, **, ***: $p<0.05$, $p<0.01$, $p<0.001$ respectively.

Table 4: The EGTI histology scoring using median (IQR)

	Control	Calc-treated	Glyc-treated	Glyc+Calc-treated
Tubular	0.0(0.0)	0.0(0.0)	3(1)[a,b]	1(1.75)[c]
Glomerular	0.0(0.0)	0.0(0.0)	2(1)[a,b]	1(1)[c]
Endothelial	0.0(0.0)	0.0(0.0)	2(1.50)[a,b]	1(1)[c]
Interstitial	0.0(0.0)	0.0(0.0)	3(1)[a,b]	1(1.75)[c]

Calc; calcitriol-treated, Glyc; glycerol-treated, Glyc+Calc; glycrol+calcitriol-treated a: significant versus control group, b: significant versus Calc-treated groups, c: significant versus Glyc-treated group at $p<0.05$.

Fig.(1)

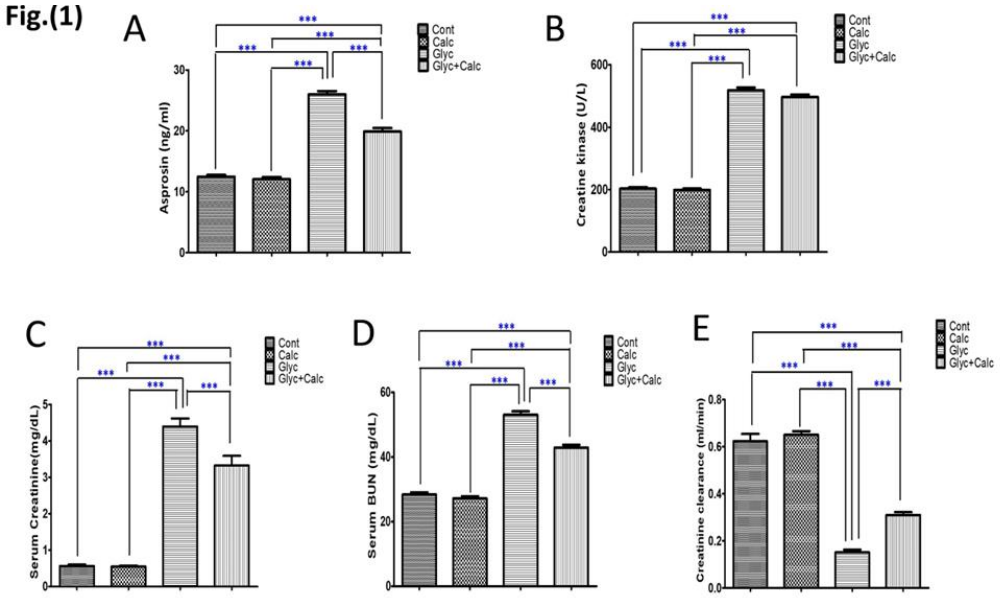

Figure 1: Bar graphs showing changes in (A): serum asprosin, (B): serum creatine kinase, (C): serum creatinine, (D): serum BUN; blood urea nitrogen and (E): creatinine clearance in all studied groups: Cont; control, Calc; calcitriol-treated, Glyc; glycerol-treated and Glyc+Calc; glycrol+calcitriol-treated. Data are represented as the mean ± SE, ***: $p<0.001$.

Fig.(2)

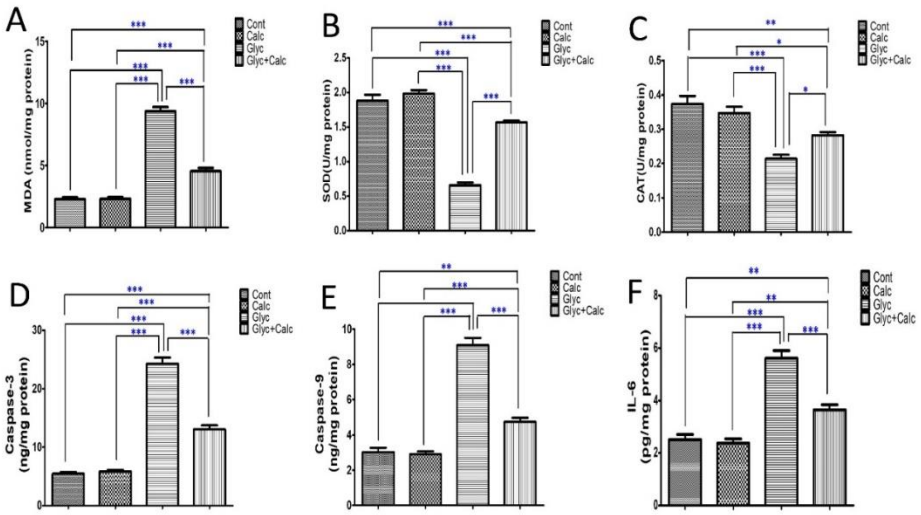

Figure 2: Bar graphs showing changes in renal tissue concentrations of (A): MDA; malondialdehyde, (B): SOD; superoxide dismutase, (C): CAT; catalase, (D): caspase-3, (E): caspase-9 and (F): IL-6; interleukin-6 in all studied groups: Cont; control, Calc; calcitriol-treated, Glyc; glycerol-treated and Glyc+Calc; glycrol+calcitriol-treated. Data are represented as the mean ± SE. *, **, ***: $p<0.05$, $p<0.01$, $p<0.001$ respectively

Fig.(3)

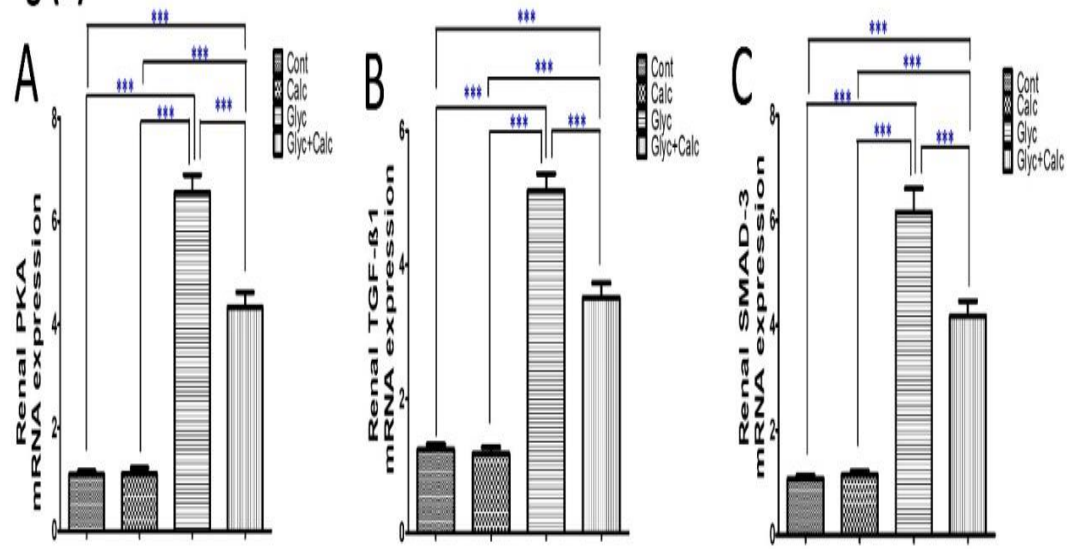

Figure 3: Bar graphs showing changes in renal tissue mRNA expression levels of (A): PKA; protein kinase A, (B): TGF-β1; transforming growth factor beta 1 , (C): SMAD-3 in all studied groups: Cont; control, Calc; calcitriol-treated, Glyc; glycerol-treated and Glyc+Calc; glycrol+calcitriol-treated. Data are represented as the mean ± SE, ***: $p<0.001$.

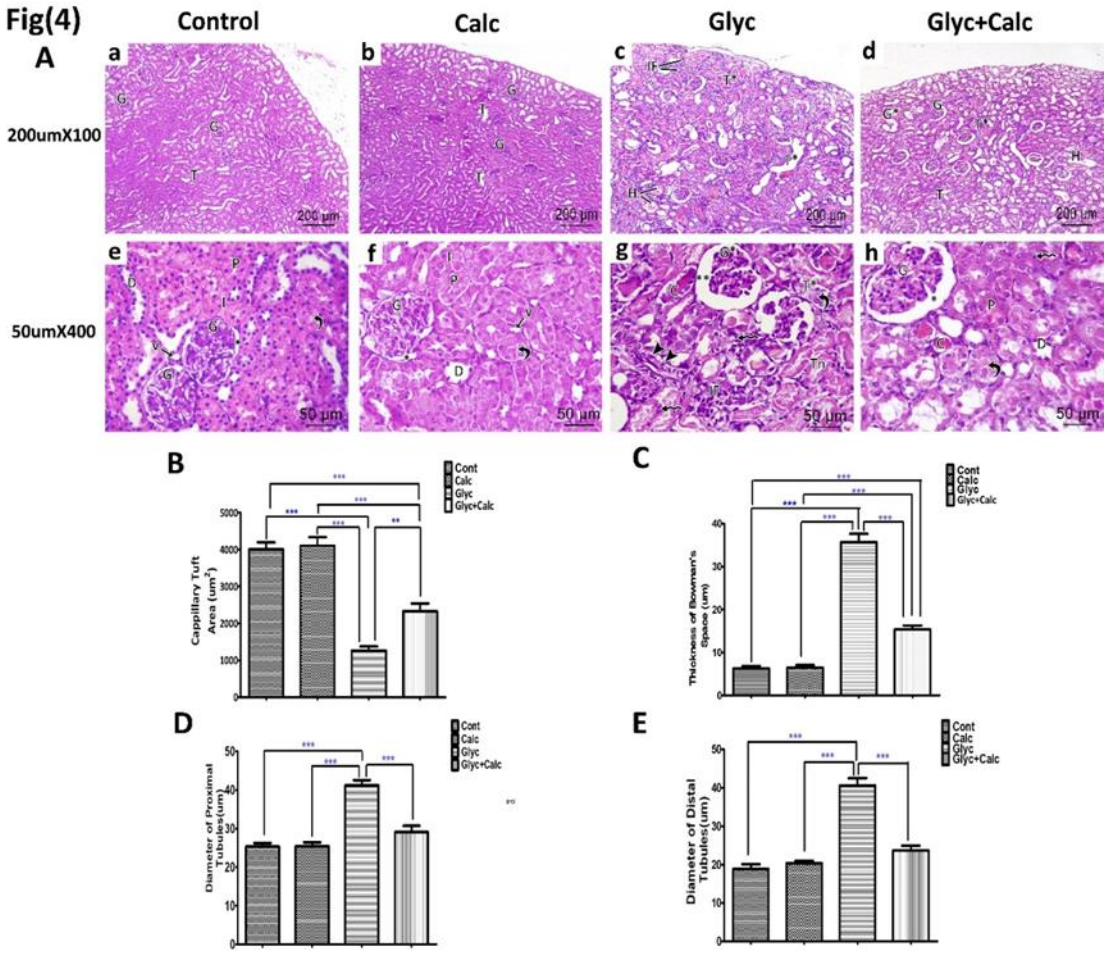

Figure 4: (A) Hematoxylin and eosin-stained sections of renal cortex of control group. (a,e); show normal glomeruli (G) surrounded by narrow Bowman's space (*). Normal cortical tubules (T) including proximal convoluted tubules (P) with intact brush border (curved arrow)and distal convoluted tubules (D). The interstitium(I) shows normal blood vessel (v).(b,f); Calc-treated group shows normal tubules (T) that formed of distal convoluted tubules (D) and proximal ones (P) with intact brush borders(curved arrows). Normal glomeruli (G) bounded by normal Bowman's space (*) and intact interstitium (I) appeared with blood vessel (v). (c,g); Glyc-treated group demonstrates shrunken segmented glomeruli (G*) with wide Bowman's spaces(**). Some tubules appear distorted (T*) with absence of their brush border (curved arrows) and hyaline casts (C) obliterate their lumen. Other ones appear necrotic (Tn). The interstitium shows infiltrating inflammatory cells (IF), areas of hemorrhage (H) and dark stained pyknotic nuclei (zigzag arrows). Notice thickened wall blood vessel within the interstitium (arrow heads). (d,h); Glyc+ Calc-treated group shows that most of glomeruli (G) appear normal, the Bowman's space (*) is about normal except for few glomeruli still showing distortion (G*). Nearly normal tubules (T) including proximal tubules (P) with their intact brush border (curved arrows) and some distal convoluted tubules (D) are normal. Few tubules (T*) still reveal casts (C) within their lumina and dark stained nuclei (zigzag arrows) in their cells. Nearly normal interstitium are seen except for some apoptotic nuclei (zigzag arrows) and few areas of hemorrhage (H). Morphometric measurements charts of (B); Capillary tuft area (um^2), (C); thickness of Bowman's spaces (um), (D); diameter of proximal convoluted tubules (um) and (E); diameter of distal convoluted tubules of rats. Cont; control, Calc; calcitriol-treated, Glyc; glycerol-treated, Glyc+Calc; glycrol+calcitriol-treated. *, **, ***: $p<0.05$, $p<0.01$, $p<0.001$ respectively. Scale bar = 200um x100 and 50 µm, x400

Fig.(5)

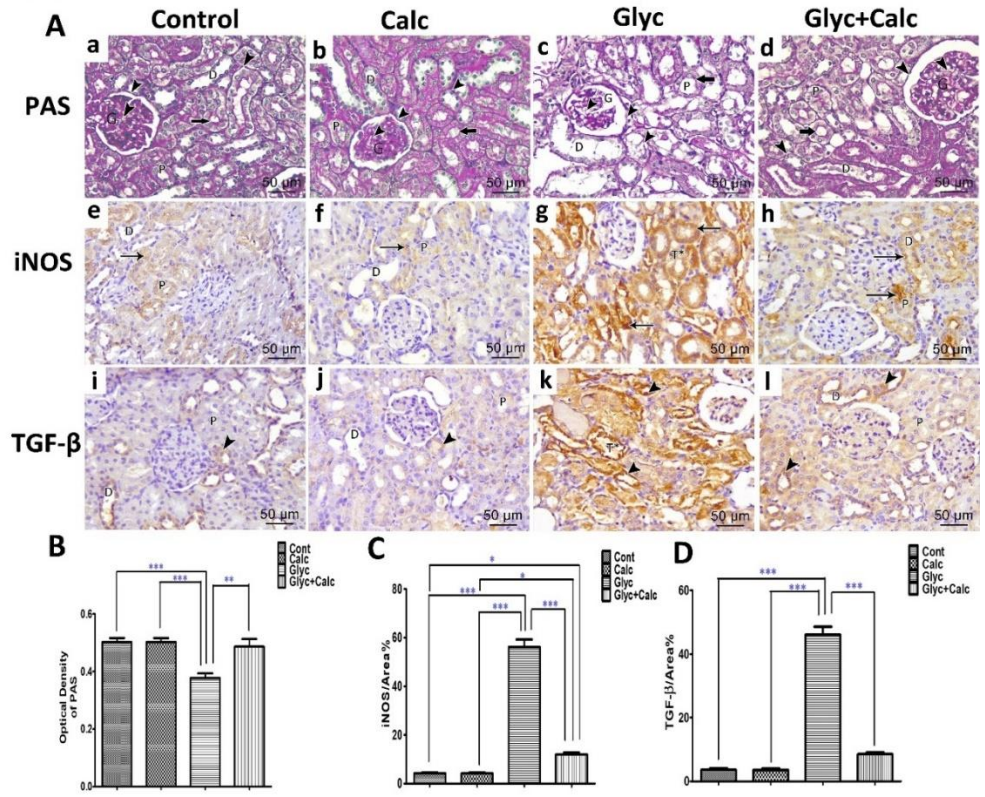

Figure 5: Representative images (A) showing: PAS reaction; Arrow heads signifying basement membranes of glomeruli (G), proximal (P),distal convoluted tubules (D) and distorted tubules(T*). Thick arrows marking brush border of proximal convoluted tubules (P). iNOS immune-positive cells expression; Arrows signifying dark brown staining of immune-positive cells. TGF-β immune-positive cells expression; Arrow heads signifying dark brown staining of immune-positive cells. (B, C, D) Charts showing the quantitative analysis of the optical density of PAS and % area of iNOS and TGF-β immune-positive reaction respectively. PAS: Periodic acid Schiff reaction, iNOS: inducible nitric oxide synthase, TGF-β: transforming growth factor-beta, Cont; control, Calc; calcitriol-treated, Glyc; glycerol-treated, Glyc+Calc; glycrol+calcitriol-treated. *, **, ***: $p<0.05$, $p<0.01$, $p<0.001$ respectively. Scale bar = 50 µm, x400

DISCUSSION

The current study discovered for the first time that serum asprosin and its dependent downstream PKA/TGF-β1/SMAD-3 signaling pathway in renal tissues were increased in glycerol-treated rat model of rhabdomyolysis accompanied by deterioration of renal functions. Pretreatment with calcitriol decreased serum asprosin and its dependent molecular pathways and protected against marked renal injury induced by glycerol.

Rhabdomyolysis is a disorder characterized by skeletal muscle breakdown, which causes leakage of myoglobin, electrolytes, and intracellular proteins into the blood stream and is mostly complicated by AKI and electrolyte disturbance [1]. The occurrence of rhabdomyolysis in glycerol-treated rats in the present study was proven by the finding of increased serum creatine kinase levels in comparison to control rats, besides the appearance of hyaline casts obliterating the lumina of renal tubules in stained renal sections, which indicates muscle damage and myoglobin release. These findings are consistent with previous studies [18,21,26] that used glycerol for the induction of rhabdomyolysis. The present study also found that pretreatment with calcitriol induced an insignificant reduction in creatine kinase serum levels compared with glycerol-treated rats; a finding that comes in line with a previous report by Reis et al. [18]. In contrast to our finding, Tsai et al. [21] reported that creatine kinase levels were significantly reduced in rats co-treated with glycerol and calcitriol in comparison to glycerol-treated rats.

AKI is the most serious complication of rhabdomyolysis [2]. The current study demonstrated worsening in renal function in glycerol-treated rats, as evidenced by increased serum levels of BUN and creatinine as well as decreased creatinine clearance. Also, the morphological results confirmed the existence of renal structural damage. These findings are in harmony with the previous studies that used the same glycerol model [5, 27]. Vitamin D deficiency

was considered a risk factor for AKI and has been reported to correlate with the severity of AKI [28] and to aggravate tubulointerstitial injury and fibrosis [29]. The current work revealed that calcitriol protected against renal injury and significantly improved renal functional parameters, improved the histopathological findings both at the level of the brush border of the tubular system and the interstitial compartment, and also improved the tubular injury score in comparison to glycerol-treated group. The protective action of calcitriol in the rhabdomyolysis model was reported in previous studies [18, 21].

Several studies demonstrated the potential central and peripheral effects of the novel adipocytokine asprosin [30,31]. Recently, the expression of asprosin in kidney tissues was reported [8]. Many studies demonstrated the changes in asprosin levels and their association with renal function in diabetic nephropathy cases that involved several pathogenic mechanisms [9-11]. The present study is the first in demonstrating the changes in asprosin levels in a rhabdomyolysis-induced AKI rat model. We found that asprosin levels were significantly increased in glycerol-treated rats compared with control rats. The present study couldn't find any significant association between asprosin levels and renal functional parameters or creatine kinase. In contrast to our finding, a previous study revealed a significant correlation between serum asprosin levels and renal function in patients with diabetic nephropathy [10]. This disparity could be explained by the difference in the studied model and its chronicity as the model in our study is acute.

The relation between calcitriol and asprosin was introduced by recent studies, which reported that calcitriol deficiency is inversely correlated with asprosin levels [32, 33]. Here, we found that calcitriol pretreatment resulted in a reduction of asprosin serum levels compared with glycerol-treated rats.

Oxidative stress was considered a keystone for AKI initiation and progression in glycerol-induced models [34]. Our study revealed significant increased levels of the oxidative marker MDA in the renal tissues of glycerol-treated rats compared to control rats, while the levels of the anti-oxidant markers SOD and catalase were significantly decreased. Also, we found that pretreatment with calcitriol protected against the development of AKI based on the finding of diminished MDA levels and up-regulation of SOD and catalase levels in renal tissues compared to glycerol group. These findings are in harmony with previously published data concerning the anti-oxidant effect of calcitriol in glycerol-induced model of AKI [18]. Asprosin was reported to have an essential role in oxidative stress [30]. Here, we found a significant positive correlation between serum asprosin levels and MDA levels in renal tissues, while it was negatively correlated with SOD and catalase levels.

Besides the pivotal role of oxidative stress in AKI pathogenesis, it was suggested that it could worsen renal dysfunction through inducing apoptotic cell death [35]. It was demonstrated that apoptosis and necrosis affect cells in the distal portion of the PCT in AKI [36]. Our study revealed up-regulation of the levels of the apoptotic markers caspase-3 and caspase-9 in the renal tissues of glycerol-treated rats compared to control rats. This finding was confirmed by the histological results that revealed faint PAS-positive reaction at the basal lamina of the glomerular capillary endothelium, tubular cells, and an interrupted brush border of PCT in glycerol-treated group. Consistent with these results, several studies implicated tubular apoptosis in renal dysfunction induced by glycerol [5,26]. Pretreatment with calcitriol significantly reduced the levels of the former apoptotic proteins, and ameliorated renal pathological changes, a finding that comes in line with the anti-apoptotic effect previously reported for calcitriol in glycerol-induced model of AKI [18].

Our study revealed a significant positive correlation between serum levels of asprosin and renal tissue levels of caspase-3 and caspase-9 in both glycerol-treated and calciriol+glycerol-treated rats. Our finding comes in line with Lee et al. [37] who reported that asprosin treatment augmented caspase-3 activity and reduced the viability of MIN6 cells. The inflammatory response has been considered a keystone in the pathogenesis of AKI and several immune and inflammatory factors has been implicated [38,39]. In the current study, we evaluated the inflammatory response by measuring the renal tissue levels of IL-6 and we found a significant increase in its levels in glycerol-treated rats in comparison to control rats. This result is compatible with the finding of Li et al. [26] who reported a marked increase in the levels of IL-6 protein in the same model.

Additionally, the present study demonstrated a strong positive iNOS immunoreaction in the cytoplasm of renal tubular cells and some capillary endothelial cells in glycerol-treated rats compared with control rats. iNOS and nitric oxide levels were reported to have a critical role in tubular cell injury via increasing lipid peroxidation and protein nitration [40]. Moreover, nitric oxide was shown to

activate NF-κB, leading to increased production of pro-inflammatory cytokines [41].

Vitamin D deficiency was reported to trigger a pro-inflammatory response, leading to renal damage and fibrosis [29]. Many studies demonstrated that calcitriol serum levels were negatively correlated with renal pro-inflammatory biomarkers and that serum levels of IL-6 were improved with calcitriol treatment [42]. Our research revealed that calcitriol pretreatment decreased the renal tissue levels of IL-6 concurrently with decreased iNOS immunoreactivity in tubular cells. So, the present study suggests that the anti-inflammatory effect of calcitriol can be attributed to inhibition of iNOS, which consequently decreases the release of inflammatory cytokines. These findings are in accordance with the previously reported protective role of calcitriol against AKI via suppressing the inflammatory response [18,21].

Our data revealed a significant positive correlation between serum levels of asprosin and renal tissue levels of IL-6 in both glycerol-treated and calciriol+glycerol-treated rats. This finding is supported by a recently published report about the pro-inflammatory effect of asprosin based on the finding that in vivo administration of recombinant asprosin in rats significantly augmented the circulating levels of IL-6 and TNF-α. Also, the in vitro studies revealed up regulation of IL-6 and TNF-α expression following treatment with asprosin [43].

The pro-fibrotic factor, TGF-β is profusely expressed in kidney tissue and has a basic role in the development of renal fibrosis [44]. Moreover, TGF-β/Smad3 signaling pathway was reported to be up-regulated in a post-contrast-induced AKI model with subsequent increased collagen IVa gene expression and apoptotic cell death [45]. The source of TGF-β in AKI was reported to be M2 macrophages. The increased production of M2 macrophages-derived TGF-β was suggested to induce collagen deposition and other extracellular matrix components causing kidney fibrosis [46]. Additionally, it was found that TGF-β activation promoted activation of SMAD-3 and caspase-1 stimulators that aggravated the AKI leading to renal fibrosis [47].

TGF-β1, the most plentiful isomer of TGF-β, is widely expressed in all renal cell types and has several properties that involve cellular proliferation and differentiation, autophagy, production of extracellular matrix and apoptosis. The active TGF-β1 was reported to bind to type II TGF-β receptor leading to phosphorylation of SMAD-2, and SMAD-3 [48]. It was reported that SMAD-3 is markedly up-regulated in fibrotic kidney diseases and models and was demonstrated to promote collagen production, inhibiting the extracellular matrix degradation, and triggering renal fibrosis [49]. Furthermore, the cAMP-PKA signaling pathway was reported to directly trigger TGF-β1 and its dependent fibrogenetic molecules production in embryonic kidney cysts [50].

According to our results, which are in line with earlier studies, rats supplied with glycerol had significantly higher levels of mRNA expression of PKA, TGF-β1, and SMAD-3 when compared to control rats. While, the expression levels were significantly down-regulated by calcitriol pretreatment in Glyc+Calc-treated group as compared to Glyc-treated rats. Also, the immunohistochemical studies revealed a strong positive TGF-β reaction in glycerol-treated rats compared with control rats, which was significantly decreased in calcitriol pre-treated rats compared with glycerol-treated rats. Consistent with our results, it was previously documented that TGF-β1 protein levels were increased in glycerol-treated rats [13]. Moreover, the nephro-protective effect of calcitriol from fibrosis in diabetic nephropathy was shown to be mediated via inhibition of TGF-β1 [19]. Also, the anti-fibrotic effect of vitamin D3 in chronic kidney disease was attributed to TGF-β1/SMAD-3 signaling pathway inhibition [51]. Additionally, calcitriol was reported to regulate EndoMT in bronchial epithelial cells via inhibiting TGF-β1 and TGF-β2 [52].

On the other hand, Gu et al. [53] reported that long lasting exposure to high levels of TGF-β negatively regulated renal inflammation. Alternately, in our study, the short-term elevated levels of TGF-β induced by glycerol injection were accompanied by elevated levels of oxidative stress, inflammation, and apoptosis. This discrepancy might be explained by the difference in the chronicity of the studied model, as the model in our study is acute.

The present study found a positive correlation between serum levels of asprosin and mRNA expression levels of PKA, TGF-β1, and SMAD-3 in renal tissues in both glycerol-treated and calciriol+glycerol-treated rats. These findings led the present study to suggest that asprosin is a crucial factor in the pathogenesis of AKI through its dependent downstream signaling pathway. Consistent with our finding, asprosin was reported to increase PKA activity in hepatic tissues [54]. Additionally, aerobic exercise was demonstrated to decrease asprosin-dependent PKA/TGF-β pathway in the liver of type 1 diabetic rats [16]. Asprosin was also suggested to directly promote EndoMT which contributes to diabetic peripheral artery

disease via TGF-β signaling pathway activation [15].

CONCLUSIONS

The present study revealed for the first time that serum levels of asprosin are increased in a rhabdomyolysis-induced AKI rat model accompanied by increased renal tissue levels of apoptotic, inflammatory and oxidative stress parameters and augmented expression of PKA-TGF-β1-SMAD-3 signaling pathway that triggered the AKI. Calcitriol pretreatment protected against glycerol-induced AKI via suppressing serum asprosin levels and its downstream-dependent pathogenic signaling pathways. So, the present study suggests the use of serum asprosin as a novel diagnostic biomarker for rhabdomyolysis-induced AKI. Developing of anti-asprosin medications might be a promising target to guard against AKI in cases of rhabdomyolysis.

DECLARATION OF INTEREST

No conflicts of interest.

FUNDING INFORMATION

This research did not receive any specific grant from funding agencies in the public, commercial, or not-for-profit sectors.

REFERENCES

1. Bagley WH, Yang H, Shah KH. Rhabdomyolysis. Intern Emerg Med. 2007 Oct;2(3):210-8. doi: 10.1007/s11739-007-0060-8. Epub 2007 Oct 1. PMID: 17909702.
2. Kasaoka S, Todani M, Kaneko T, Kawamura Y, Oda Y, Tsuruta R, et al. Peak value of blood myoglobin predicts acute renal failure induced by rhabdomyolysis. J Crit Care. 2010 Dec; 25(4): 601-4. doi: 10.1016/j.jcrc. 2010.04.002. PMID: 20537502.
3. Bosch X, Poch E, Grau JM. Rhabdomyolysis and acute kidney injury. N Engl J Med. 2009 Jul 2;361(1):62-72. doi: 10.1056/NEJMra0801327. Erratum in: N Engl J Med. 2011 May 19;364(20):1982. PMID: 19571284.
4. Nara A, Yajima D, Nagasawa S, Abe H, Hoshioka Y, Iwase H. Evaluations of lipid peroxidation and inflammation in short-term glycerol-induced acute kidney injury in rats. Clin Exp Pharmacol Physiol. 2016 Nov;43(11):1080-6. doi: 10.1111/1440-1681.12633. PMID: 27529136.
5. Al Asmari AK, Al Sadoon KT, Obaid AA, Yesunayagam D, Tariq M. Protective effect of quinacrine against glycerol-induced acute kidney injury in rats. BMC Nephrol. 2017 Jan 28;18(1):41. doi: 10.1186/s12882-017-0450-8. PMID: 28129740; PMCID: PMC5273840.
6. Romere C, Duerrschmid C, Bournat J, Constable P, Jain M, Xia F, et al. Asprosin, a Fasting-Induced Glucogenic Protein Hormone. Cell. 2016 Apr 21;165(3):566-79. doi: 10.1016/j.cell.2016.02.063. Epub 2016 Apr 14. PMID: 27087445; PMCID: PMC4852710.
7. Hoffmann JG, Xie W, Chopra AR. Energy Regulation Mechanism and Therapeutic Potential of Asprosin. Diabetes. 2020 Apr;69(4):559-66. doi: 10.2337/dbi19-0009. PMID: 32198197; PMCID: PMC7085243.
8. Kocaman N, Kuloğlu T. Expression of asprosin in rat hepatic, renal, heart, gastric, testicular and brain tissues and its changes in a streptozotocin-induced diabetes mellitus model. Tissue Cell. 2020 Oct; 66:101397. doi: 10.1016/j.tice.2020.101397. Epub 2020 Jun 5. PMID: 32933720.
9. Goodarzi G, Setayesh L, Fadaei R, Khamseh ME, Aliakbari F, Hosseini J, et al. Circulating levels of asprosin and its association with insulin resistance and renal function in patients with type 2 diabetes mellitus and diabetic nephropathy. Mol Biol Rep. 2021 Jul;48(7):5443-50. doi: 10.1007/s11033-021-06551-2. Epub 2021 Jul 25. PMID: 34304366.
10. Wang R, Lin P, Sun H, Hu W. Increased serum asprosin is correlated with diabetic nephropathy. Diabetol Metab Syndr. 2021 May 1;13(1):51. doi: 10.1186/s13098-021-00668-x. PMID: 33933135; PMCID: PMC8088566.
11. Xu L, Cui J, Li M, Wu Q, Liu M, Xu M, et al. Association Between Serum Asprosin and Diabetic Nephropathy in Patients with Type 2 Diabetes Mellitus in the Community: A Cross-Sectional Study. Diabetes Metab Syndr Obes. 2022 Jun 18;15: 1877-84. doi: 10.2147/DMSO.S361808. PMID: 35757196; PMCID: PMC9215350.
12. Zeisberg M, Hanai J, Sugimoto H, Mammoto T, Charytan D, Strutz F, et al. BMP-7 counteracts TGF-beta1-induced epithelial-to-mesenchymal transition and reverses chronic renal injury. Nat Med. 2003 Jul;9(7):964-8. doi: 10.1038/nm888. PMID: 12808448.
13. Korrapati MC, Shaner BE, Schnellmann RG. Recovery from glycerol-induced acute kidney injury is accelerated by suramin. J Pharmacol Exp Ther. 2012 Apr;341(1):126-36. doi: 10.1124/jpet.111.190249. Epub 2012 Jan 6. PMID: 22228809; PMCID: PMC3310704.
14. Zeng R, Han M, Luo Y, Li C, Pei G, Liao W, et al. Role of Sema4C in TGF-β1-induced mitogen-activated protein kinase activation and epithelial-mesenchymal transition in renal tubular epithelial cells. Nephrol Dial Transplant. 2011 Apr;26(4):1149-56. doi: 10.1093/ndt/gfq619. Epub 2010 Oct 19. PMID: 20959347; PMCID: PMC3070071.
15. You M, Liu Y, Wang B, Li L, Zhang H, He H, et al. Asprosin induces vascular endothelial-to-mesenchymal transition in diabetic lower extremity peripheral artery disease. Cardiovasc Diabetol. 2022 Feb 15;21(1):25. doi: 10.1186/s12933-022-01457-0. PMID: 35168605; PMCID: PMC8848671.
16. Ko JR, Seo DY, Kim TN, Park SH, Kwak HB, Ko KS, et al. Aerobic Exercise Training Decreases Hepatic Asprosin in Diabetic Rats. J Clin Med.

2019 May 12;8(5):666. doi: 10.3390/jcm8050666. PMID: 31083617; PMCID: PMC6572469.
17. Tan X, Li Y, Liu Y. Paricalcitol attenuates renal interstitial fibrosis in obstructive nephropathy. J Am Soc Nephrol. 2006 Dec;17(12):3382-93. doi: 10.1681/ASN.2006050520. Epub 2006 Nov 2. PMID: 17082242.
18. Reis NG, Francescato HDC, de Almeida LF, Silva CGAD, Costa RS, Coimbra TM. Protective effect of calcitriol on rhabdomyolysis-induced acute kidney injury in rats. Sci Rep. 2019 May 8;9(1):7090. doi: 10.1038/s41598-019-43564-1. PMID: 31068635; PMCID: PMC6506495.
19. Yu R, Mao J, Yang Y, Zhang Y, Tian Y, Zhu J. Protective effects of calcitriol on diabetic nephropathy are mediated by down regulation of TGF-β1 and CIP4 in diabetic nephropathy rat. Int J Clin Exp Pathol. 2015 Apr 1;8(4):3503-12. PMID: 26097534; PMCID: PMC4466921.
20. Kapil A, Singh JP, Kaur T, Singh B, Singh AP. Involvement of peroxisome proliferator-activated receptor gamma in vitamin D-mediated protection against acute kidney injury in rats. J Surg Res. 2013 Dec;185(2):774-83. doi: 10.1016/j.jss.2013.07.017. Epub 2013 Jul 30. PMID: 24011919.
21. Tsai J, Lee C, Hsieh Y, Hsu B. Calcitriol ameliorated rhabdomyolysis induced acute renal failure in rats. Int J Clin Exp Med. 2017;10(2):2430-9 www.ijcem.com /ISSN:1940-5901/IJCEM0044787.
22. El-Kashef DH, Sharawy MH. Venlafaxine mitigates cisplatin-induced nephrotoxicity via down-regulating apoptotic pathway in rats. Chem Biol Interact. 2018 Jun 25; 290:110-8. doi: 10.1016/j.cbi.2018.05.015. Epub 2018 May 29. PMID: 29852128.
23. Kiernan JA. Histological and Histochemical Methods. Theory and Practice, 5th edition. Scion Publishing Ltd, Banbury, UK. 2015; pp: 1-137.
24. Suvarna SK, Layton C, Bancroft JD. Bancroft's theory and practice of histological techniques, 7th edition. Elsevier Health sciences, Churchill Livingstone. 2013; pp: 492- 538.
25. Khalid U, Pino-Chavez G, Nesargikar P, Jenkins RH, Bowen T, Fraser DJ, et al. Kidney ischaemia reperfusion injury in the rat: the EGTI scoring system as a valid and reliable tool for histological assessment. J Histol Histopathol. 2016; 3(1):1. https://doi.org/ 10.7243/2055-091x-3-1
26. Li YF, Xu BY, An R, Du XF, Yu K, Sun JH, et al. Protective effect of anisodamine in rats with glycerol-induced acute kidney injury. BMC Nephrol. 2019 Jun 17;20(1):223. doi: 10.1186/s12882-019-1394-y. PMID: 31208365; PMCID: PMC6580578.
27. Sharawy MH, Abdelrahman RS, El-Kashef DH. Agmatine attenuates rhabdomyolysis-induced acute kidney injury in rats in a dose dependent manner. Life Sci. 2018 Sep 1; 208:79-86. doi: 10.1016/j.lfs.2018.07.019. Epub 2018 Jul 17. PMID: 30009822.
28. Luchi WM, Shimizu MH, Canale D, Gois PH, de Bragança AC, Volpini RA, et al. Vitamin D deficiency is a potential risk factor for contrast-induced nephropathy. Am J Physiol Regul Integr Comp Physiol. 2015 Aug 1;309(3): R215-22. doi: 10.1152/ajpregu.00526.2014. Epub 2015 Jun 3. PMID: 26041113.
29. Gonçalves JG, de Bragança AC, Canale D, Shimizu MH, Sanches TR, Moysés RM, et al. Vitamin D deficiency aggravates chronic kidney disease progression after ischemic acute kidney injury. PLoS One. 2014 Sep 15;9(9): e107228. doi: 10.1371/journal.pone.0107228. PMID: 25222475; PMCID: PMC4164619.
30. Zhang Z, Tan Y, Zhu L, Zhang B, Feng P, Gao E, et al. Asprosin improves the survival of mesenchymal stromal cells in myocardial infarction by inhibiting apoptosis via the activated ERK1/2-SOD2 pathway. Life Sci. 2019 Aug 15; 231:116554. doi: 10.1016/j.lfs.2019.116554. Epub 2019 Jun 10. PMID: 31194992.
31. Ke F, Xue G, Jiang X, Li F, Lai X, Zhang M, et al. Combination of asprosin and adiponectin as a novel marker for diagnosing non-alcoholic fatty liver disease. Cytokine. 2020 Oct; 134:155184. doi: 10.1016/j.cyto.2020.155184. Epub 2020 Jul 6. PMID: 32645536.
32. Buczyńska A, Sidorkiewicz I, Ławicki S, Krętowski AJ, Zbucka-Krętowska M. Prenatal Screening of Trisomy 21: Could Oxidative Stress Markers Play a Role? J Clin Med. 2021 May 28;10(11):2382. doi: 10.3390/jcm10112382. PMID: 34071365; PMCID: PMC8198847.
33. Mohammed SA, Allwsh TA. Study interplay between Asprosin with Vitamin D in metabolic syndrome. J Contemp Med Sci. 2022 Dec; 8(6), 395–9. https://doi.org/10.22317/jcms.v8i6.1300
34. Guo SX, Zhou HL, Huang CL, You CG, Fang Q, Wu P, et al. Astaxanthin attenuates early acute kidney injury following severe burns in rats by ameliorating oxidative stress and mitochondrial-related apoptosis. Mar Drugs. 2015 Apr 13;13(4):2105-23. doi: 10.3390/md13042105. PMID: 25871290; PMCID: PMC4413202.
35. Wagener FA, Dekker D, Berden JH, Scharstuhl A, van der Vlag J. The role of reactive oxygen species in apoptosis of the diabetic kidney. Apoptosis. 2009 Dec;14(12):1451-8. doi: 10.1007/s10495-009-0359-1. PMID: 19466552; PMCID: PMC2773115.
36. Linkermann A, Himmerkus N, Rölver L, Keyser KA, Steen P, Bräsen JH, et al. Renal tubular Fas ligand mediates fratricide in cisplatin-induced acute kidney failure. Kidney Int. 2011 Jan;79(2):169-78. doi: 10.1038/ki.2010.317. Epub 2010 Sep 1. PMID: 20811331.
37. Lee T, Yun S, Jeong JH, Jung TW. Asprosin impairs insulin secretion in response to glucose and viability through TLR4/JNK-mediated inflammation. Mol Cell Endocrinol. 2019 Apr 15; 486:96-104. doi: 10.1016/j.mce.2019.03.001. Epub 2019 Mar 7. PMID: 30853600.

38. Karwasra R, Kalra P, Gupta YK, Saini D, Kumar A, Singh S. Antioxidant and anti-inflammatory potential of pomegranate rind extract to ameliorate cisplatin-induced acute kidney injury. Food Funct. 2016 Jul 13;7(7):3091-101. doi: 10.1039/c6fo00188b. PMID: 27273121.
39. Ruiz-Andres O, Suarez-Alvarez B, Sánchez-Ramos C, Monsalve M, Sanchez-Niño MD, Ruiz-Ortega M, et al. The inflammatory cytokine TWEAK decreases PGC-1α expression and mitochondrial function in acute kidney injury. Kidney Int. 2016 Feb;89(2):399-410. doi: 10.1038/ki.2015.332. PMID: 26535995.
40. El-Awady MS, Suddek GM. Agmatine ameliorates atherosclerosis progression and endothelial dysfunction in high cholesterol-fed rabbits. J Pharm Pharmacol. 2014 Jun;66(6):835-43. doi: 10.1111/jphp.12204. Epub 2014 Jan 7. PMID: 24393128.
41. El-Kashef DH. Role of venlafaxine in prevention of cyclophosphamide-induced lung toxicity and airway hyperactivity in rats. Environ Toxicol Pharmacol. 2018 Mar; 58:70-6. doi: 10.1016/j.etap.2017.12.020. Epub 2017 Dec 27. PMID: 29306104.
42. Mao L, Ji F, Liu Y, Zhang W, Ma X. Calcitriol plays a protective role in diabetic nephropathy through anti-inflammatory effects. Int J Clin Exp Med. 2014 Dec 15;7(12):5437-44. PMID: 25664053; PMCID: PMC4307500.
43. Huang Q, Chen S, Xiong X, Yin T, Zhang Y, Zeng G, et al. Asprosin Exacerbates Endothelium Inflammation Induced by Hyperlipidemia Through Activating IKKβ-NF-κBp65 Pathway. Inflammation. 2023 Apr;46(2):623-38. doi: 10.1007/s10753-022-01761-7. Epub 2022 Nov 19. PMID: 36401667.
44. Su J, Morgani SM, David CJ, Wang Q, Er EE, Huang YH, et al. TGF-β orchestrates fibrogenic and developmental EMTs via the RAS effector RREB1. Nature. 2020 Jan;577(7791):566-71. doi: 10.1038/s41586-019-1897-5. Epub 2020 Jan 8. Erratum in: Nature. 2020 Jan 15; PMID: 31915377; PMCID: PMC7450666.
45. Kilari S, Yang B, Sharma A, McCall DL, Misra S. Increased transforming growth factor beta (TGF-β) and pSMAD3 signaling in a Murine Model for Contrast Induced Kidney Injury. Sci Rep. 2018 Apr 26;8(1):6630. doi: 10.1038/s41598-018-24340-z. PMID: 29700311; PMCID: PMC5919895.
46. Lu J, Cao Q, Zheng D, Sun Y, Wang C, Yu X, et al. Discrete functions of M2a and M2c macrophage subsets determine their relative efficacy in treating chronic kidney disease. Kidney Int. 2013 Oct;84(4):745-55. doi: 10.1038/ki.2013.135. Epub 2013 May 1. PMID: 23636175.
47. Sun J, Ge X, Wang Y, Niu L, Tang L, Pan S. USF2 knockdown downregulates THBS1 to inhibit the TGF-β signaling pathway and reduce pyroptosis in sepsis-induced acute kidney injury. Pharmacol Res. 2022 Feb; 176:105962. doi: 10.1016/j.phrs.2021.105962. Epub 2021 Oct 28. PMID: 34756923.
48. Meng XM, Chung AC, Lan HY. Role of the TGF-β/BMP-7/Smad pathways in renal diseases. Clin Sci (Lond). 2013 Feb;124(4):243-54. doi: 10.1042/CS20120252. PMID: 23126427.
49. Yuan W, Varga J. Transforming growth factor-beta repression of matrix metalloproteinase-1 in dermal fibroblasts involves Smad3. J Biol Chem. 2001 Oct 19;276(42):38502-10. doi: 10.1074/jbc.M107081200. Epub 2001 Aug 13. PMID: 11502752.
50. Weng L, Wang W, Su X, Huang Y, Su L, Liu M, et al. The Effect of cAMP-PKA Activation on TGF-β1-Induced Profibrotic Signaling. Cell Physiol Biochem. 2015;36(5):1911-27. doi: 10.1159/000430160. Epub 2015 Jul 17. PMID: 26202352.
51. Wang F, Hu R, Zhang J, Pei T, He Z, Ju L, et al. High-dose vitamin D3 supplementation ameliorates renal fibrosis by vitamin D receptor activation and inhibiting TGF-β1/Smad3 signaling pathway in 5/6 nephrectomized rats. Eur J Pharmacol. 2021 Sep 15; 907:174271. doi: 10.1016/j.ejphar.2021.174271. Epub 2021 Jun 17. PMID: 34147475.
52. Fischer KD, Agrawal DK. Vitamin D regulating TGF-β induced epithelial-mesenchymal transition. Respir Res. 2014 Nov 21;15(1):146. doi: 10.1186/s12931-014-0146-6. Erratum in: Respir Res. 2015; 16:139. PMID: 25413472; PMCID: PMC4245846.
53. Gu YY, Liu XS, Huang XR, Yu XQ, Lan HY. Diverse Role of TGF-β in Kidney Disease. Front Cell Dev Biol. 2020 Feb 28; 8:123. doi: 10.3389/fcell.2020.00123. PMID: 32258028; PMCID: PMC7093020.
54. He L, Chang E, Peng J, An H, McMillin SM, Radovick S, et al. Activation of the cAMP-PKA pathway Antagonizes Metformin Suppression of Hepatic Glucose Production. J Biol Chem. 2016 May 13;291(20):10562-70. doi: 10.1074/jbc.M116.719666. Epub 2016 Mar 21. PMID: 27002150; PMCID: PMC4865906.

To Cite:
Khalil, S., Abd El-Fatah, S., Fathy, M., Elwany, N., Ahmad, E., Mohamed, N., Habib, M. Asprosin, a prospective biomarker for rhabdomyolysis-induced acute kidney damage in rats: involvement of PKA/TGF-β1/SMAD-3 signaling pathway. *Zagazig University Medical Journal*, 2023; (1146-1160): -. doi: 10.21608/zumj.2023.209146.2796